Molecular Alterations in a High-Fat Mouse Model Before the Onset of Diet–Induced Nonalcoholic Fatty Liver Disease

Sangwon Lee[1], Sangmin Lee[1], Won Sunwoo[1], Taehoon Kim[1], Kyumin Lee[1], and Ja Kyung Kim[2]

[1]Sehwa High School, Seoul, Republic of Korea

[2]Department of Internal Medicine, Yonsei University College of Medicine, Seoul, Republic of Korea

Summary

Nonalcoholic fatty liver disease (NAFLD) is one of the most prevalent chronic liver diseases worldwide. However, the precise mechanism of the disease and a definitive treatment has not yet been discovered. Studies on NAFLD frequently use an animal model fed a high-fat diet (HFD) for 24 to 48 weeks. While full-blown liver inflammation and fibrosis occur after 24 weeks of HFD administration, changes in the liver at earlier time points have not been rigorously investigated. We hypothesized that there would be some molecular alterations at an earlier time point that would predict the later onset of pathologic symptoms. The aim of our study was to delineate the changes that take place before the pathologically detectable NAFLD appears in HFD mice, which would facilitate more effective study and treatment of NAFLD. We fed C57BL/6 mice a high-fat diet for 8 to 24 weeks and evaluated liver fat accumulation, inflammation, and fibrosis. Significant pathologic fat content, inflammation, and fibrosis in the liver could only be noticed after 24 weeks of HFD. However, we observed dysregulated immune function as early as 8 weeks after the start of the diet, and detected molecular changes associated with fat accumulation by week 12. Symptoms related to liver fibrosis were the most delayed changes. Our results suggest that alterations in inflammation and fat metabolism are early changes, followed by liver fibrosis in the HFD-induced NAFLD animal model. Therefore, future NAFLD experiments using this model can be designed to include earlier time points at which the desired HFD-induced alterations occur, and NAFLD experiments that aim to investigate immunologic alterations may be performed after a shorter duration of HFD feeding.

Introduction

Nonalcoholic fatty liver disease (NAFLD) is one of the most prevalent chronic liver diseases worldwide. It is excessive fat accumulation not caused by alcohol in hepatic cells, which leads to severe liver inflammation and advanced liver cirrhosis (1-3). Although excessive accumulation of fat in the liver is generally considered the hallmark of NAFLD, inflammation and liver fibrosis are regarded as more significant prognostic factors that determine the fate of the disease (4-6).

The liver regulates the balance between energy generation from food sources and energy storage according to the tissue requirements. For example, the liver maintains normal lipid metabolism by taking up and synthesizing fatty acids, and then secreting them in the form of triglycerides (TG) (7). NAFLD is believed to be a result of poor regulation in the liver of this energy homeostasis. One of the most important peptide hormones in energy homeostasis is insulin. Insulin controls the glucose level throughout the body by suppressing glucose metabolism in the liver. However, it is reported that this function of insulin may be hindered by increased hepatic TG content (8). The process of fatty acid and TG synthesis in the liver, called lipogenesis, is elaborately controlled by several molecules. Sterol regulatory element binding proteins (SREBPs) can be up-regulated by insulin and facilitate lipogenesis. Enzymes including fatty acid synthase (FAS) and stearoyl-CoA desaturase (SCD) also play a direct role in *de novo* lipogenesis (9).

While excess fat accumulation in the liver may cause no further symptoms, when the changes in NAFLD lead to inflammation and liver fibrosis, poorer prognoses such as total liver failure can occur (4). The exact mechanism that leads from simple fatty liver disease to inflammation and cirrhosis has not been completely elucidated. It has been suggested that once increase in fat content occurs due to metabolic alterations, various stimuli may trigger liver inflammation. For example, transforming necrosis factor (TNF)-α levels increase, and regulatory immune cells such as forkhead box P3 (Foxp3)-positive cells are suppressed; thus intensifying further inflammatory activities (10, 11). Repeated liver injury can activate hepatic stellate cells, the main cellular component in the production of fibrous tissue, resulting in the accumulation of fibrous collagen fibers. The tensile strength of accumulated extracellular matrix (ECM) is further strengthened through the molecular crosslinking of collagen. This process is facilitated by enzymes in the

lysyl oxidase (LOX) family (12, 13).

Even with the current knowledge on NAFLD, the pathogenesis of NAFLD requires further investigation in order to offer treatments other than lifestyle modification through diet and exercise (14). Animal models of NAFLD are valuable for elucidating the pathogenesis and for examining the therapeutic effects of various treatments. The liver of NAFLD animals should contain fat accumulation, inflammation, and ideally fibrosis. Since there seems to be a strong link between diet, metabolic syndrome, and NAFLD; the majority of the animal models focus on providing a diet that causes these damages.

The standard method to generate NAFLD animal models is to feed mice a diet high in fat and sucrose content. The ideal duration of feeding is yet to be defined, although longer feeding times result in more severe inflammatory and fibrous changes (15). Nevertheless, feeding mice for an extended period of time requires a lot of resources and research time. Therefore, we were curious about the effect of a reduced time span for the development of NAFLD, so that time and resources might be saved in NAFLD experiments.

We fed C57BL/6 mice a high-fat diet (HFD) for 8 to 24 weeks and evaluated the changes in the liver with respect to fat accumulation, inflammation, and fibrosis. Significant pathologic fat accumulation, inflammation and fibrosis in the liver could only be noticed after 24 weeks of HFD. However, dysregulated immune function was noticed as early as 8 weeks after the start of the diet, whereas the molecular changes associated with the fat accumulation was detected at 12 weeks. Evidence of liver fibrosis were the latest changes to emerge after the start of HFD. Our results suggest that alterations in inflammation and fat metabolism can be detected earlier than liver fibrosis in the NAFLD animal model developed by feeding a HFD.

Results
Evaluating changes in liver fat content

Mice given a high-fat diet (HFD) for 24 weeks had a mean body weight of 41.9 ± 3.03g, while mice fed a standard diet weighed 32.33 ± 1.15g. There was a significant difference between the two groups ($p = 0.007$) **(Figure 1)**.

We evaluated fat content by scoring the percentage of H&E stained hepatocytes that contained fat vesicles (grade 0: none, grade 1: <25%, grade 2: 26–50%, grade 3: 51–75%, grade 4: 76–100%). Significant fat tissue changes were noticed after 24 weeks of HFD (2.60 ± 0.245), compared to normal tissue specimens (0.00 ± 0.000) that were harvested from mice fed a standard diet for 24 weeks **(Figure 2A)**. Fat changes were also estimated by measuring the triglyceride (TG) content of the liver tissue. Giving HFD resulted in significantly
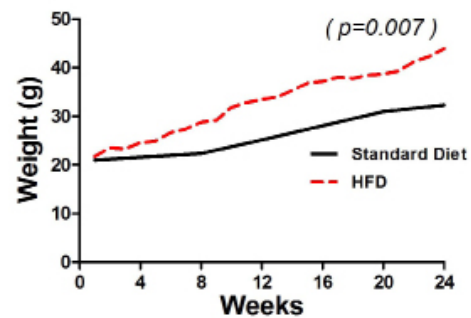

Figure 1: Changes in body weight during a standard diet versus high-fat diet (HFD).

increased liver TG content after 24 weeks (66.84 ± 2.65 mg/g protein), as compared to mice fed with a standard diet (44.29 ± 7.37 mg/g protein) **(Figure 2B)**.

Although pathologically noticeable fat changes in the liver were detected only after 24 weeks of HFD, we investigated whether molecular changes that might assist fat accumulation could be detected at earlier time points. We performed quantitative real-time polymerase chain reaction (RT-PCR) on the mRNA of *SREBP-1c*, a gene that could trigger lipogenesis, *FAS*, a gene that catalyzes fatty acid synthesis, and *SCD*, a gene that converts saturated fatty acid to unsaturated fatty acid. The expression was compared to that of animals fed with the standard diet for 24 weeks. Increased *SREBP-1c* expression was noticed by week 12 (5.94 ± 0.88 fold change) **(Figure 2C)**, but the incremental increase in the expression of *SREBP-1c* was largest at week 24 (34.41 ± 5.05 fold change), showing statistical significance. In addition, the expression of *SCD* started to increase by week 12 (3.25 ± 0.40 fold change) **(Figure 2C)**. However, the change in week 24 (4.58 ± 0.50 fold change) was not significant when compared with that of week 12. There was no significant change in *FAS* mRNA expression during HFD **(Figure 2C)**.

Evaluating changes in liver inflammation

Evaluation of liver inflammation was done after H&E staining by counting inflammatory foci in 20 consecutive high-power fields. Significant pathologic inflammation was detectable after 24 weeks of HFD (2.80 ± 0.20 foci), compared to normal tissue specimens (0.00 ± 0.00 foci) that were harvested from mice fed with a standard diet for 24 weeks **(Figure 3A)**. In association with liver inflammation, we evaluated the expression of *FOXP3* mRNA, which is a relatively specific marker for regulatory T cells, which are known to control and suppress liver inflammation (16). Surprisingly, *FOXP3* mRNA expression was suppressed as early as 8 weeks (0.056 ± 0.02 fold change) after the start of HFD, before
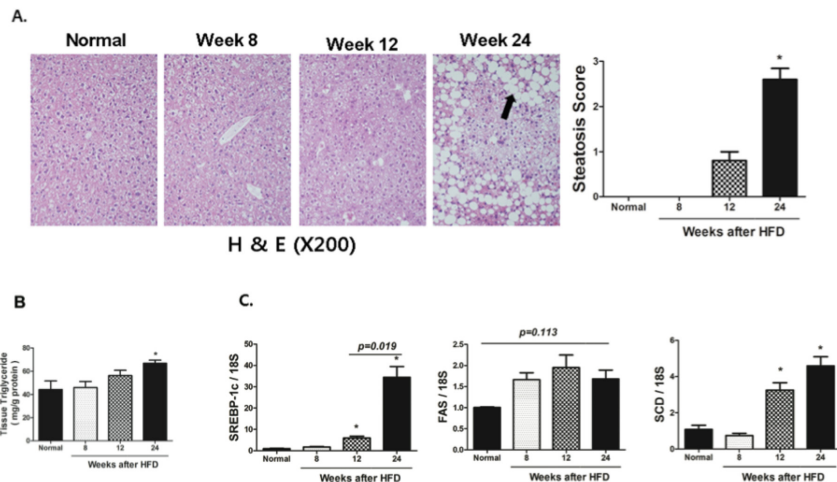
Figure 2: Fat accumulation in the liver. (A) A representative picture of the liver with H&E staining (200X) and the evaluation of fat accumulation. The accumulation was scored as the percentage of hepatocytes containing fat vesicles (grade 0: none, grade 1: <25%, grade 2: 26–50%, grade 3: 51–75%, grade 4: 76–100%). A representative area of fat accumulation is indicated by a black arrow. (B) Evaluation of liver tissue triglyceride (TG) content. (C) Changes in the expression of the following genes related to liver fat accumulation: *SREBP-1c*, which triggers lipogenesis; *FAS*, which catalyzes fatty acid synthesis; and *SCD*, which converts saturated fatty acid to unsaturated fatty acid. *$p < 0.05$, when compared with that of the normal liver, harvested after 24 weeks of a standard diet. **$p < 0.05$ when compared with the HFD-fed liver specimen, harvested the previous week.

the changes of other molecular markers related to fat accumulation were present **(Figure 3B)**. The expression of *TNF-α*, a cytokine involved in systemic inflammation, was increased from week 12 (13.74 ± 1.54 fold change) through week 24 (15.87 ± fold change) **(Figure 3B)**.

Evaluating changes in liver fibrosis

Histological assessment of liver fibrosis was performed after Sirius Red staining using an image analysis system. The area of Sirius Red–stained collagen fibers was calculated. Significant formation of fibrous tissue was found after 24 weeks of HFD (1.51 ± 0.16 %) **(Figure 4A)**. The expression of *collagen α1(I)* (*col1α(I)*) mRNA, a marker for collagen fibers, was elevated at week 12 (5.74 ± 0.98 fold change) through 24 (18.05 ± 1.77 fold change), earlier than the pathologic changes **(Figure 4B)**. However, *smooth muscle α-actin* (*αSMA*) mRNA, a marker for activated hepatic stellate cells, which are the main cellular component that produce collagen fibers in the liver, were increased by week 24 (14.24 ± 1.37 fold change) **(Figure 4B)**. The expression of *LOXL2*, which facilitates the crosslinking of collagen so as to consolidate ECM, also increased by week 24 (3.50 ± 0.71 fold change) **(Figure 4B)**.

Discussion

In this experiment, we compared the liver specimens of mice fed an HFD for 8, 12 and 24 weeks with those of mice fed a standard diet for 24 weeks. We performed histological evaluation in terms of the fat accumulation, inflammation, and fibrosis. We also

investigated the molecular changes on genes related with lipid metabolism, fibrosis and inflammation. The study demonstrated that molecular changes leading to NAFLD start as early as 8 weeks after the start of HFD, while pathologically noticeable NAFLD can be achieved only after 24 weeks of HFD administration. Among the molecular changes, suppressed regulatory T cells, identified by decreased *FOXP3* mRNA expression, were present first and followed by altered expression of genes related to lipogenesis and inflammatory cytokines. This suggests that alterations in inflammation and fat metabolism can be detected earlier than liver fibrosis in the NAFLD animal model developed by feeding HFD.

The most popular theory of the mechanism of NAFLD is the "2-hit" hypothesis (10). It suggests that the accumulation of free fatty acids and TG's in the liver is the first hit. The second hit may come from oxidative stress, the production of inflammatory cytokines, and alterations in the immune system. Among these factors, immune regulation of cytokine production is thought to be particularly important (16). In a previous study, depleting regulatory T cells led to increased inflammatory cytokine production and aggravated NAFLD (16). In our study, regulatory T cell suppression was present before other molecular and pathological changes in liver fat production were detected, at 8 weeks after HFD. The inhibited regulatory T cell function was followed by increased production of the inflammatory cytokine TNF-α and liver fat synthesis, as detected by elevated *SREBP-1c* and *SCD* expression. It seems that actual accumulation of excessive fat in the liver might
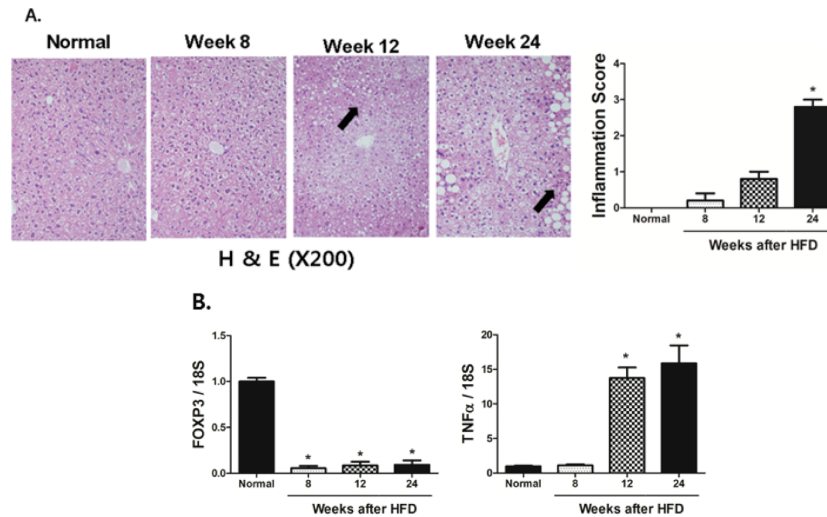
Figure 3: Liver inflammation. (A) Evaluation of liver inflammation after H&E staining. Inflammatory foci were counted in 20 consecutive high-power fields (40X objective) (average histological grade, grade 0: no foci, grade 1: <2 foci per high-power field, grade 2: ≥2 foci per high-power field). Representative inflammatory foci are indicated by a black arrow. (B) Changes in the expression of genes related to liver inflammation: *FOXP3*, a marker for regulatory T cells known to control and suppress liver inflammation and *TNF-α*, a cytokine involved in systemic inflammation. *$p < 0.05$, when compared with that of the normal liver, harvest after 24 weeks of a standard diet. **$p < 0.05$ when compared with the HFD-fed liver specimen, harvested on the previous week.
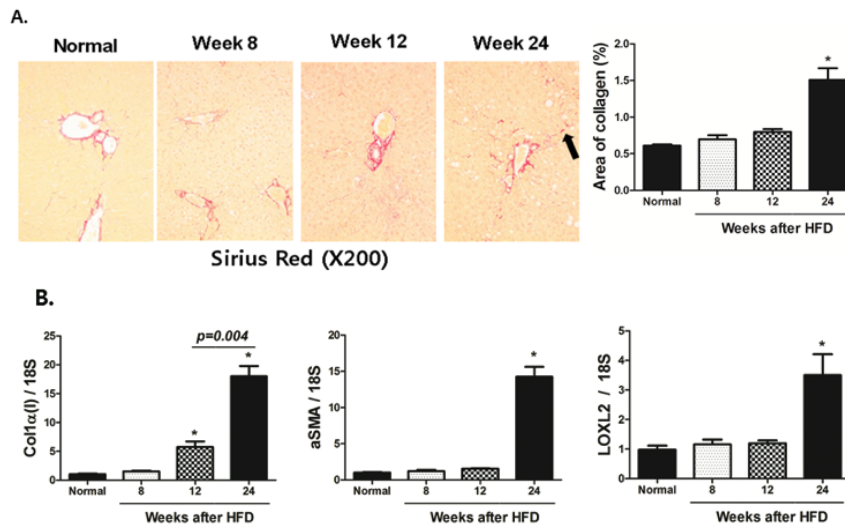
not always be necessary in order to trigger immunologic abnormalities. We believe that over-production of fat in the body itself might be triggering regulatory T cell dysfunction, thereby producing inflammatory cytokines. The precise role of excessive fat inflow and initiation of regulatory T cell dysfunction should be studied in more elaborate experiments in which the function of regulatory T cells is evaluated by more direct means.

Liver fibrosis results from repeated liver insult and inflammation (3). In our study, liver fibrosis was found after 24 weeks of HFD, similar to the other pathological abnormalities. On the other hand, molecular changes that suggest an increased amount of liver collagen fiber, estimated by quantification of *col1α(I)* mRNA, were noticed after 12 weeks of HFD. Increased *LOXL2* expression, which might play a role in the consolidation of the ECM, increased at week 24 after the production of excessive collagen fibers. According to previous studies, hepatic stellate cells are activated at the beginning of the fibrosis event, and *αSMA* is the marker of these activated hepatic stellate cells (17). Interestingly, in our investigation, even though *col1α(I)* expression started to increase at week 12, a significant increase in *αSMA* expression was not present until week 24. Although a precise explanation for this result cannot be made from this study, we believe that since hepatic stellate cells make up a very small portion of liver cells, activation and proliferation of these cells at the beginning might have not been obvious enough to make any significant difference. However, delayed *αSMA* up-regulation in

our study should be verified by other means such as immunohistochemical study of hepatic stellate cell activation.

Our study compared liver tissue of mice fed an HFD for 8, 12 and 24 weeks with those of mice fed a standard diet for 24 weeks. Therefore, one of the limitations of our study is that the comparison was only made with mice fed a standard diet for 24 weeks instead of for each corresponding time point. There is very little scientific evidence to suggest that aging mice have the same level of liver fat accumulation, inflammation, or fibrosis as younger mice.

In our study, the administration of HFD, which induces surplus fat in the body, resulted in suppressed regulatory T cells before a significant accumulation of TG in the liver could be detected. It seems that changes associated with generation and progression of NAFLD may not always follow the typical sequence of inflammation and then liver fibrosis. Abnormal fat synthesis and storage may instead induce changes related with inflammation and fibrosis in a very short time and all the alterations take place within a short interval. This result indicates that a NAFLD experiment using the HFD mouse model can be designed according to the object of the study, and NAFLD experiments that aim to investigate immunologic alterations may be achieved with a shorter duration of HFD feeding.

Figure 4: Liver fibrosis. (A) A representative picture of the liver with Sirius Red staining (100X). Percent region of fibrosis was determined after Sirius Red staining by calculating the fibrosis ratio using an image analysis system. A representative stained part is indicated by a black arrow. (B) Changes in the expression of genes related to liver fibrosis: *collagen α1(I)* (*col1α(I)*), a marker for collagen fibers, *smooth muscle α-actin* (*αSMA*), a marker for activated hepatic stellate cells, and *LOXL2*, which facilitates crosslinking of collagen so as to consolidate the ECM. *$p < 0.05$, when compared with that of the normal liver, harvested after 24 weeks of a standard diet. **$p < 0.05$ when compared with the HFD-fed liver specimen, harvested on the previous week.

Methods

Animals

The experimental procedures and protocols were approved by the Institutional Animal Care and Use Committee (IACUC) of Gangnam Severance Hospital, Yonsei University College of Medicine. The study was carried out in accordance with the recommendations and restrictions of the IACUC (permit number: 2013-0173-1).

Male C57BL/6 mice at 8 weeks of age were obtained from the Central Lab Animal Inc. (Seoul, Korea) and housed with a 12 hour light-dark cycle. The mice were fed with either standard diet or HFD that consisted of 15% anhydrous milk fat, 1.0% cholesterol, and 50% sucrose. The mice fed with standard diet (n = 5) were sacrificed and their livers were harvested after 24 weeks. The mice fed with HFD were sacrificed 8 (n = 5), 12 (n = 5), or 24 (n = 5) weeks after the start of the diet. A portion of fresh liver tissue was fixed in 10% buffered formalin, and the remaining tissue was snap-frozen in liquid nitrogen and stored at −80°C.

Histological Evaluation

Sections of liver tissue fixed in 10% formalin and embedded in paraffin wax were stained with H&E and Sirius Red for histological evaluation. A pathologist, blinded to the study, assessed the slides for fat accumulation, inflammation, and fibrosis, as in previous studies (18-20), with minor modifications. Fat accumulation was scored as the percentage of

hepatocytes containing fat vesicles (grade 0: none, grade 1: <25%, grade 2: 26–50%, grade 3: 51–75%, grade 4: 76–100%). Inflammation was histologically quantified by counting inflammatory foci in 20 consecutive high-power fields (40X objective) (average histological grade, grade 0: no foci, grade 1: <2 foci per high-power field, grade 2: ≥2 foci per high-power field).

The area of collagen was calculated using an image analysis system as described by a previous study (21) with some modifications. Images of Sirius Red–stained sections were captured with a 10X magnification. The stain colors the fibrosis area as red and the parenchyma as grey. After the image was converted into a binary image, the 2-dimensinal patterns were measured by direct pixel counting on the binary images. The total area was the sum of the area of microscopic fields including parenchyma and fibrosis. For each slide, the area of fibrosis was evaluated in 20 consecutive high-power fields and averaged.

RNA Extraction and Gene Expression Analysis

Total RNA was extracted from the frozen whole liver using Trizol reagent (Invitrogen, Carlsbad, CA, USA) according to the manufacturer's protocol. RNA samples were quantified by spectrophotometry. The RNA integrity was assessed using agarose gel electrophoresis and ethidium bromide staining. The RNA samples were then diluted in RNase-free water and stored at −70°C until use. Five micrograms of RNA were reverse-transcribed using RNA PCR kit version 1.2

(Takara Bio Inc, Japan) according to the manufacturer's recommendations. We used the oligonucleotide primers and TaqMan probes for the following genes, with 18S as an internal control: *collagen α1(I) (col1α(I)), smooth muscle α-actin (αSMA) lysyl oxidase homolog (LOXL2), tumor necrosis factor (TNF)-α, FOXP3, sterol regulatory binding protein (SREBP)-1c, fatty acid synthase (FAS),* and *stearoyl-CoA desaturase (SCD)*. The probes were obtained from Applied Biosystems (Perkin-Elmer/PE Applied Biosystems, Forster City, CA, USA), purchased in a ready-for-use form as Assays-on-Demand Gene Expression Products. The TaqMan probes were labeled at the 5' end with the reporter dye FAM and minor groove binder (MGB) non-fluorescent quencher on the 3'end. The quantitative PCR was performed in triplicate for each sample on a Step One Plus Real Time System (Applied Biosystems). Each 20-μL reaction contained 10 μL of TaqMan Fast Universal Master Mix (Applied Biosystems, Darmstadt, Germany), 1 μL of Gene Expression Mix, and 2 μL of cDNA diluted in 7 μL RNase-free water. The thermal cycler conditions were 20 seconds at 95°C , and 40 cycles of 5 seconds at 95°C followed by 20 seconds at 60°C. Fold change in mRNA expression of target genes relative to the endogenous 18S control were calculated as done in previous studies (22).

Assessment of Tissue Triglyceride (TG) Content

Hepatic TG content was quantified using a commercial kit (ab65336, Abcam, Cambridge, MA, USA) according to the manufacturer's recommendations. Briefly, lipid extracts were prepared by the homogenization of 50 mg of frozen liver tissue in a solution of 5% NP-40. The homogenized tissue was heated to 80–100°C in a water bath for 2–5 minutes, then cooled down to room temperature. The samples were purified and diluted.

Data Analysis

All results are shown as means ± standard error of mean (SEM). Data were analyzed by nonparametric analysis (Kruskal-Wallis or Mann-Whitney test) or one-way ANOVA with Tukey's post hoc analysis. $p < 0.05$ was considered statistically significant. All calculations were performed with SPSS version 15.0 software for Windows (SPSS Inc., Chicago, IL, USA).

References

1. Angulo P. GI Epidemiology: nonalcoholic fatty liver disease. *Aliment Pharm Therap.* 2007;25(8):883-9.
2. Argo CK, Caldwell SH. Epidemiology and natural history of non-alcoholic steatohepatitis. *Clin Liver Dis.* 2009;13(4):511-31.
3. Angulo P. Long-Term Mortality in Nonalcoholic Fatty Liver Disease: Is Liver Histology of Any Prognostic Significance? *Hepatology.* 2010;51(2):373-5.
4. Harrison SA, Torgerson S, Hayashi PH. The natural history of nonalcoholic fatty liver disease: a clinical histopathological study. *Am J Gastroenterol.* 2003;98(9):2042-7.
5. Fassio E, Alvarez E, Dominguez N, Landeira G, Longo C. Natural history of nonalcoholic steatohepatitis: A longitudinal study of repeat liver biopsies. *Hepatology.* 2004;40(4):820-6.
6. Adams LA, Sanderson S, Lindor KD, Angulo P. The histological course of nonalcoholic fatty liver disease: a longitudinal study of 103 patients with sequential liver biopsies. *J Hepatol.* 2005;42(1):132-8.
7. Fabbrini E, Magkos F. Hepatic steatosis as a marker of metabolic dysfunction. *Nutrients.* 2015;7(6):4995-5019.
8. Samuel VT, Liu ZX, Qu X, Elder BD, Bilz S, Befroy D, et al. Mechanism of hepatic insulin resistance in non-alcoholic fatty liver disease. J Biol Chem. 2004;279(31):32345-53.
9. Ameer F, Scandiuzzi L, Hasnain S, Kalbacher H, Zaidi N. *De novo* lipogenesis in health and disease. *Metabolism.* 2014;63(7):895-902.
10. Day CP, Saksena S. Non-alcoholic steatohepatitis: definitions and pathogenesis. *J Gastroenterol Hepatol.* 2002;17 Suppl 3:S377-84.
11. Marra F, Gastaldelli A, Svegliati Baroni G, Tell G, Tiribelli C. Molecular basis and mechanisms of progression of non-alcoholic steatohepatitis. *Trends Mol Med.* 2008;14(2):72-81.
12. Wang SX, Mure M, Medzihradszky KF, Burlingame AL, Brown DE, Dooley DM, et al. A crosslinked cofactor in lysyl oxidase: redox function for amino acid side chains. *Science.* 1996;273(5278):1078-84.
13. Smith-Mungo LI, Kagan HM. Lysyl oxidase: properties, regulation and multiple functions in biology. *Journal of the International Society for Matrix Biology.* 1998;16(7):387-98.
14. Cohen JC, Horton JD, Hobbs HH. Human fatty liver disease: old questions and new insights. *Science.* 2011;332(6037):1519-23.
15. Hebbard L, George J. Animal models of nonalcoholic fatty liver disease. *Nat Rev Gastroenterol Hepatol.* 2011;8(1):35-44.
16. Ma X, Hua J, Mohamood AR, Hamad AR, Ravi R, Li Z. A high-fat diet and regulatory T cells influence susceptibility to endotoxin-induced liver injury. *Hepatology.* 2007;46(5):1519-29.
17. Li JT, Liao ZX, Ping J, Xu D, Wang H. Molecular mechanism of hepatic stellate cell activation and antifibrotic therapeutic strategies. *J Gastroenterol.* 2008;43(6):419-28.
18. Brunt EM. Nonalcoholic steatohepatitis: Definition and pathology. *Semin Liver Dis.* 2001;21(1):3-16.
19. Kirsch R, Clarkson V, Shephard EG, Marais DA,

Jaffer MA, Woodburne VE, et al. Rodent nutritional model of non-alcoholic steatohepatitis: Species, strain and sex difference studies. *J Gastroen Hepatol.* 2003;18(11):1272-82.

20. Kleiner DE, Brunt EM, Van Natta M, Behling C, Contos MJ, Cummings OW, et al. Design and validation of a histological scoring system for nonalcoholic fatty liver disease. *Hepatology.* 2005;41(6):1313-21.

21. O'Brien MJ, Keating NM, Elderiny S, Cerda S, Keaveny AP, Afdhal NH, et al. An assessment of digital image analysis to measure fibrosis in liver biopsy specimens of patients with chronic hepatitis C. Am J Clin Pathol. 2000;114(5):712-8.

22. Livak KJ, Schmittgen TD. Analysis of relative gene expression data using real-time quantitative PCR and the 2(-Delta Delta C(T)) Method. Methods. 2001;25(4):402-8.